Field dependence of the magnetic quantum phase transition in MnSi

1997 J. Phys.: Condens. Matter 9 6677

(http://iopscience.iop.org/0953-8984/9/31/019)

J. Phys.: Condens. Matter **9** (1997) 6677–6687. Printed in the UK PII: S0953-8984(97)80595-4

Field dependence of the magnetic quantum phase transition in MnSi

C Thessieu, C Pfleiderer†, A N Stepanov and J Flouquet
DRFMC-SPSMS, CEA Grenoble, 38054 Grenoble Cédex 9, France

Received 3 January 1997, in final form 4 April 1997

Abstract. The dependence on pressure (P) and field (H) of the magnetic phase diagram of MnSi has been investigated by means of measurements of the AC susceptibility (χ) up to 16 kbar and 7 T at temperatures down to 30 mK. For ambient pressure, we report on a peak in χ above T_c at a characteristic temperature T_m that rises quickly with field. The pressure dependence of T_m is found to be strongly analogous to that of the zero-field transition to long-range order at T_c. Features of χ in the field versus temperature (T) phase diagram may be viewed as 'fingerprint' evidence of a field-induced crossover at T_m of the itinerant magnetism from a non-polarized regime at high T and low H to a polarized regime at low T and high H. The long-wavelength spin spiral, present at low H, appears to be supported only in the polarized regime, so in the immediate vicinity of the critical pressure P_c for which $T_c \to 0$, a small pocket exists as a re-entrant state.

1. Introduction

The nature of unconventional magnetic or superconducting phases of metals may be clarified by tuning them systematically with the help of an external parameter such as pressure or field. Here we present measurements on the magnetic state of MnSi at high field and high pressure, which is considered an archetypal representative of the class of weak itinerant *ferro*magnets [1, 2]. At ambient pressure, MnSi orders at a critical temperature of $T_c \approx 30$ K. Low-temperature features of its metallic state are consistent with a spectrum of fermion quasiparticle excitations of a normal Landau Fermi liquid [3, 4]. Dominant magnetic contributions to the free energy may alternatively be described on the basis of the experimentally observed spectrum of strongly enhanced *ferro*magnetic fluctuations [5, 6]. The magnetic order is, however, not exactly that of a *ferro*magnetic system, but stabilizes in its cubic B20 crystal environment the formation of a helical spin spiral along $\langle 111 \rangle$ of wavelength $\lambda \approx 180$ Å, i.e. occupying 0.01% of the volume of the Brillouin zone [7]. Neutron diffraction studies have shown that this spin spiral alters its propagation direction for fields $H > H_{c1} \approx 0.1$ T, forming a fan spiral of essentially unchanged wavelength up to $H_{c2} \approx 0.6$ T. At fields above H_{c2} it collapses [8–10].

Detailed measurements of the resistivity ρ and AC susceptibility χ have established that T_c collapses to zero for pressures in excess of $P_c \approx 14.6$ kbar [11, 12]. Although the resistivity at this pressure drops monotonically by nearly three orders of magnitude between room temperature and 20 mK in the samples investigated, it never assumes the

† Author to whom any correspondence should be addressed. Present address: Physikalisches Institut, Universität Karlsruhe, 76128 Karlsruhe, Germany; e-mail: cpfleide@fphws01.physik.uni-karlsruhe.de.

0953-8984/97/316677+11$19.50

conventional quadratic temperature dependence of a normal Landau Fermi liquid. One may instead account for the observed form of $\rho(T)$, which approaches $T^{5/3}$ in the limit of mK temperatures, by means of a quasiparticle interaction potential that is consistent with measurements of de Haas–van Alphen oscillations and the specific heat at ambient pressure [3, 13, 14]. This interpretation supposes that the effective-fermion-quasiparticle interaction at P_c is well approximated by the exchange of critical *ferro*magnetic fluctuations over the size of the Brillouin zone. Quantitative measurements of the AC susceptibility showed, however, that the transition becomes weakly first order for $P > P^* \approx 12$ kbar, before disappearing above P_c. The susceptibility of the paramagnetic regime at these pressures remains finite for $T < T^* \approx 12$ K, the location of a broad peak in χ for $P > P^*$. To date, a number of magnetic metals have been reported for which such a peak may be connected to a change of curvature of the magnetization as a function of field [15–17]. However, the role of many-body effects as regards an understanding of this behaviour remains an unsettled issue.

In the past, detailed experimental and theoretical investigations have been carried out on compounds showing rich modulated and antiferromagnetic structures [18]. We report here hence also on a study into the question of the origin of the peak in χ at T^*, and evidence on whether the magnetic state of MnSi is driven towards *antiferro*magnetism with increasing pressure.

2. Experimental procedure

The AC susceptibility of MnSi has been determined as a function of P between ambient pressure and 16 kbar. Measurements were predominantly carried out in isothermal field sweeps reaching up to 7 T in the vicinity of P_c and 1 T at all other pressures, for T in the range 30 mK $< T <$ 60 K. We have supplemented these measurements with scans for varying T at fixed H where necessary. The two samples of differing purity investigated had negligible demagnetizing factors. A single crystal of residual resistivity ratio in excess of 240 was studied at all pressures. It was oriented so that the modulation field and DC field were parallel and along $\langle 100 \rangle$. Further properties of this sample and a description of our experimental method have been reported elsewhere [3, 4, 11, 19]. A second single crystal of residual resistivity ratio around 30 was studied for comparison at ambient pressure. This sample was oriented along $\langle 111 \rangle$. Properties of samples of the latter quality have also been reported elsewhere [20].

Pressures were generated in a clamp-type pressure cell, made of BeCu and a non-magnetic AlCrNi alloy. The pressure cell was enclosed in a tightly fitting Cu screen to ensure temperature uniformity throughout, and the sample was thermally linked to the screen with the help of high-conductivity Cu wires and a carefully designed joint made of non-magnetic, high-conductivity Ag epoxy. The temperature of the thermal screen was regulated to better than 0.1% during field sweeps. Magnetic fields up to 7 T were generated with a superconducting solenoid, and field ramps carried out at digitally generated sweep rates, well below the threshold of eddy current heating.

The AC susceptibility χ was measured with the help of a carefully balanced pair of secondaries inside a small primary, all placed inside the pressure cell [11, 19]. The experiments were carried out at a modulation frequency of 80 Hz and modulation amplitudes of the order of 10^{-4} T, thus avoiding skin and eddy current effects as well as self-heating of the experimental assembly. The resulting AC signal was analysed with a digital, phase-sensitive detector, so that the in-phase response χ' and out-of-phase response χ'' could be distinguished. Calibration runs as functions of H and T for the empty susceptometer

established the absence of (i) variations of the mismatch of the pair of secondaries larger than 1%, (ii) signal contributions from the pressure cell, and (iii) interference between the signal detection system and the DC field. Additional measurements at ambient pressure at fields up to 4 T were carried out on the same samples with the help of a SQUID and another AC susceptometer.

The experiments were carried out in the sequence of (i) cooling from a temperature above 40 K, (ii) a field cycle to at least 1 T, and (iii) the T-sweep to the next temperature at zero field. As described below, no evidence was observed of irreversible behaviour above a characteristic field $H_{c2} \approx 0.6$ T. Field sweeps of increasing strength thus systematically probed the behaviour of a zero-field-cooled sample, while those of decreasing field strength probed that of a field-cooled sample.

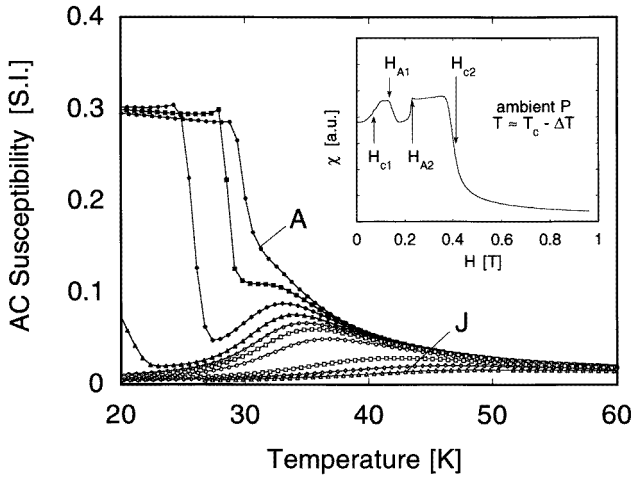

Figure 1. The AC susceptibility as function of T at fixed fields up to 4 T. At fields above 0.4 T a broad maximum develops above T_c, shifting to higher T as the field increases. The curves correspond from top to bottom to 0.3 T (A), 0.4 T, 0.5 T. 0.6 T. 0.7 T, 0.8 T, 1.0 T, 2.0 T, 3.0 T and 4.0 T (J) respectively. The inset shows a typical susceptibility trace as function of field for a temperature just below T_c. This curve representatively yields all field-related features associated with the spiral state, and is described in detail in the text.

3. Results

Shown in figure 1 are typical curves of the AC susceptibility (χ') for selected fields at ambient pressure. Further information may be obtained from isothermal field sweeps, such as that shown in the inset of figure 1. These data allow us to establish the magnetic phase diagram of MnSi at ambient pressure. We may summarize the observed behaviour as follows. At $H = 0$ T (not shown in figure 1), $\chi(T) \propto (T - T_c)^{-1}$ with $\mu_{eff} \approx 2.2\ \mu_B$/Mn up to T_c. Below T_c, $\chi(T)$ is saturated and its imaginary part is finite, as expected of a magnetically ordered regime in which magnetic domains are formed. At 0.3 T (trace A) we still observe the same general features as for zero field. However, for temperature sweeps at more elevated fields, a broad maximum at $T_m(H)$ appears. For $T > T_m$, the Curie behaviour and the corresponding effective moment of $\chi(T)$ are nevertheless unchanged. We note, however, that χ^{-1} below T_m is essentially proportional to the field for fixed temperature. We may thus consider the peak at T_m as being the temperature at which the

properties of an itinerant magnet change from those of an essentially non-polarized state (for $T > T_m$) to those of a field-polarized state (for $T < T_m$). The value of T_m, finally, increases up to the highest field investigated here, 4 T (trace J), while the overall susceptibility decreases. For $H > 0.6$ T, the imaginary part of the susceptibility is essentially negligible at all temperatures.

To obtain more detailed information on low-field features of the ordered phase, which yields a long-wavelength spin spiral as described in the introduction, it is also helpful to measure the isothermal susceptibility as a function of field. A typical curve containing all of the key features observed at ambient pressure for T just below T_c is shown in the inset of figure 1. We may in particular define four characteristic field values as follows. H_{c1} is the point of steepest initial increase, H_{A1} and H_{A2} the lower and upper bounds of a small local minimum, and H_{c2}, finally, is the point of steepest descent at higher fields. Field cycles show that χ at H_{c1} is slightly irreversible. Below H_{c2}, the imaginary part of the susceptibility is finite, but above H_{c2} it is essentially negligible. Above T_c, isothermal field variations show a maximum of χ at $H_m(T)$. We note that the characteristic lines $T_m(H)$ or $H_m(T)$ do not coincide in the H versus T phase diagram since they correspond to a broad crossover and not a sharp phase transition.

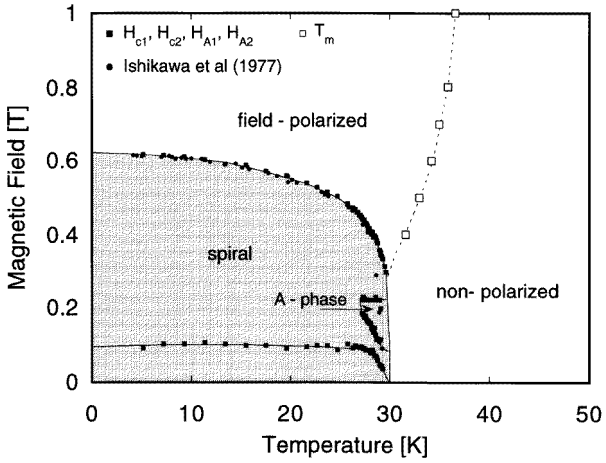

Figure 2. Comparison of the magnetic phase diagram as determined from our measurements and the neutron diffraction study by Ishikawa *et al* [9]. Excellent agreement is observed between the two methods. Also added is the variation of the peak at T_m as a function of field.

The resulting phase diagram at ambient pressure is shown in figure 2. To understand the variations of $\chi(T)$ at H_{c1}, H_{c2}, H_{A1}, and H_{A2}, we have added previous results of neutron diffraction investigations [8–10]. We note first a remarkable agreement of our values of H_{c1}, H_{c2}, H_{A1}, and H_{A2} with the transition lines of the spiral state. From this comparison, we conclude that H_{c2} coincides with the collapse of the spiral at sufficiently large field and temperature. At lower field and temperatures, it has been shown that three phases may be distinguished. Up to H_{c1} the spin spiral seems unaffected, while above H_{c1} the magnetic field induces a rotation of the propagation axes towards the field direction and a change into a fan spiral. It has to be emphasized though, that the wavelength of the spiral is found to vary little as a function of field. In the small temperature versus field pocket of the A phase, defined for $H_{A1} < H < H_{A2}$ below T_c, the propagation direction of the spiral was recently established to be rotated to a direction perpendicular to the field [21]. Away from

the spiral state, finally, we distinguish two regimes separated by the broad maximum of χ at T_m.

The agreement of our data with results of previous neutron diffraction studies at ambient pressure provides an excellent guide for establishing the magnetic phase diagram at high pressure. Up to $P^* \approx 12$ kbar, above which the transition is weakly first order, T_c drops by nearly 60% from 30 K to around 12 K. The crossover line defined via the peak at T_m is also very sensitive to the effect of pressure, and shifts rapidly to lower temperatures. However, global features of the H versus T behaviour of the spiral state below T_c, namely the absolute values of H_{c1}, H_{c2}, H_{A1}, and H_{A2}, remain essentially unaffected. It is in this context interesting to note that the size of the change of the susceptibility $\Delta\chi$ at H_{c1}, H_{c2}, H_{A1}, and H_{A2} for increasing pressure monotonically decreases somewhat, and that the anomaly associated with the A phase disappears altogether on approaching P_c. We may suppose that the susceptibility at low fields, as measured here along $\langle 100 \rangle$, arises predominantly from variations of the spin spiral either in terms of its wavelength or its orientation. However, recent neutron diffraction experiments at high pressure show that the wavelength of the spin spiral is essentially unchanged. The small decrease of $\Delta\chi$ with pressure may thus be taken as evidence of a pressure-induced rotation of the propagation direction of the spiral at zero field away from $\langle 111 \rangle$ [10, 21].

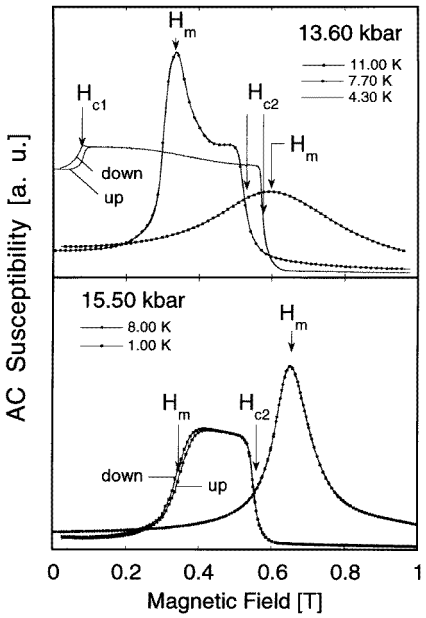

Figure 3. (a) Typical isothermal susceptibility traces at 13.60 kbar. For 4.30 K $< T_c \approx 6.45$ K, the curve resembles that measured at low P. At 7.70 K, just above T_c, we note the appearance of a peak at H_m and a little shoulder corresponding to H_{c2}. At 11.00 K, well above T_c, H_m is larger than H_{c2}, and the curve peaks only at H_m. (b) Typical isothermal susceptibility traces at 15.50 kbar (just above P_c). In both parts of the figure, small irreversibilities in field cycles have been marked. At higher T these irreversibilities disappear.

Near P_c, the susceptibility reflects a more delicately balanced situation. Examples of isothermal susceptibility curves, as measured at 13.60 kbar and 15.50 kbar, i.e. 1 kbar below and above the critical pressure, respectively, are shown in figure 3. We first describe data obtained at 13.60 kbar, for which $T_c \approx 6.45$ K. At 4.30 K, i.e. below T_c, we observe a

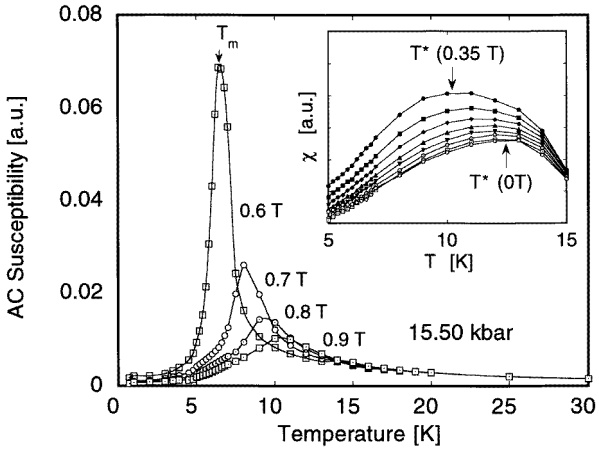

Figure 4. The T-dependence of the susceptibility as computed from the isothermal field curves. The lines are fits to the measured points. The strong field dependence of the broad peak at T_m remains, but in comparison to the behaviour seen at ambient pressure shown in figure 1, the peak is more pronounced. The inset shows the field dependence of the broad maximum at T^* at 15.50 kbar for low fields.

small initial increase of $\chi(H)$ at H_{c1} and a drop at H_{c2}. As before, the susceptibility near H_{c1} is slightly irreversible, and the imaginary part of the susceptibility becomes negligible only above H_{c2}. No evidence was observed for anomalies that may correspond to the A phase. At 7.70 K, i.e. just above T_c, the susceptibility passes first through a pronounced maximum at $H'_m > H_{c1}$, which is reminiscent of the behaviour at H_m, before dropping off at a field H_{c2}. Our measurements show furthermore that H'_m increases with T, and that the associated peak broadens and decreases. In contrast to this, the drop at H_{c2} decreases slightly with increasing T until it merges with the peak at H_m. At higher temperatures only a broad maximum at H_m remains, such as that shown here for 11.00 K.

We may now turn to data measured at $P \approx 15.50$ kbar, also shown in figure 3. At low temperature we observe typically a rapid increase of χ at a field $H'_m > H_{c1}$, and a subsequent decrease at a higher field H_{c2}, like that shown for 1.00 K. Field cycles indicate that the low-field increase of the susceptibility at H'_m is slightly hysteretic, which is supported by our observation of a non-negligible imaginary part of the susceptibility between H'_m and H_{c2}. Although a precise quantitative scaling is outside the possibilities of this experiment, we find that the susceptibility remains finite up to 7 T, and the magnetization is hence unsaturated. No anomalies are observed that could be associated with the A phase. As the temperature increases, the lower bound of the broad maximum at H'_m shifts rapidly to higher fields, and the upper bound at H_{c2} slightly drops. Above a temperature of the order of 6 K, the lower bound finally merges with the drop at H_{c2} into a broad maximum at H_m shown here for a measurement at 8.00 K. For still increasing temperature, H_m increases further while the peak broadens and the peak height decreases. At temperatures above 6.00 K, we have no further evidence for hysteretic behaviour in field cycles; however, the imaginary part of the susceptibility is slightly elevated in the vicinity of H_m. We note, in particular, that the observed features of the imaginary part of the susceptibility do not permit an integration of χ as a function of field to obtain quantitative information on the magnetization.

Prior to summarizing all of the above-described behaviour in terms of a magnetic phase diagram, the nature of the peak at H_m may be clarified with the help of $\chi(T)$ for selected

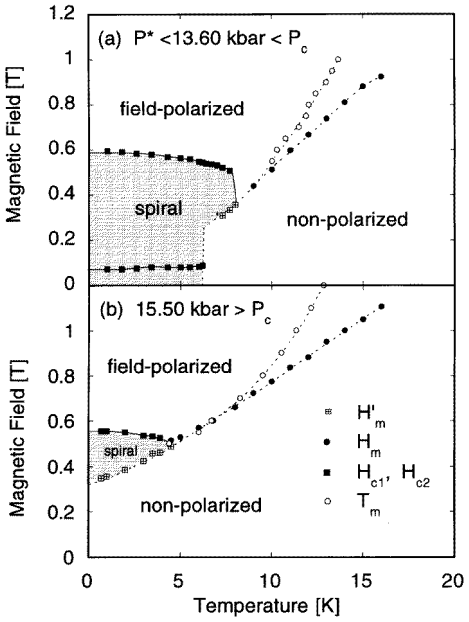

Figure 5. (a) The magnetic phase diagram at 13.60 kbar as obtained from the isothermal susceptibility traces. Just above T_c, the spiral state appears as a re-entrant phase in a small T-interval. (b) The magnetic phase diagram at 15.50 kbar. The spiral state seems to appear only as a re-entrant phase up to 5 K.

fields, as shown in figure 4. The curves shown here are guides to the eye through data points that were obtained from field sweeps in the regime of reversible behaviour. As described in the introduction, the susceptibility for a pressure of 15.50 kbar at zero field is Curie-like at high temperature, and has a broad maximum at $T^* \approx 12$ K. As shown in the inset of figure 4 this maximum shifts slightly towards lower temperatures at low fields. For intermediate fields, it is not possible to follow the evolution of this maximum further. However, as shown in the main part of figure 4, for fields of 0.5 T and higher, the susceptibility has a very pronounced maximum at a temperature T_m, of which the overall characteristics are in perfect agreement with the behaviour observed at ambient pressure, shown in figure 1.

This, finally, brings us to the magnetic phase diagrams at 13.60 kbar and 15.50 kbar, shown in figure 5. The dominating feature is a crossover line defined through the peak at T_m separating an essentially non-polarized regime at high temperature from a field-polarized regime at low temperature. The pronounced increase of χ around T_m is for these pressures sufficiently strong to be seen also in field sweeps. The dependence of $T_m(H)$, however, does not coincide with $H_m(T)$, as pointed out above, due to the broadened nature of the maximum in χ. In the low-field and low-temperature regime of this phase diagram, the spin spiral is supported only in the field-polarized regime for sufficiently low fields. For temperatures just above T_c at 13.60 kbar and low temperatures at 15.50 kbar, the spiral state exists as a re-entrant phase in field sweeps. The absolute values of H_{c1}, H_{c2}, H_{A1}, and H_{A2} are only very moderately pressure dependent. In contrast to this, T_c and T_m are strongly pressure dependent.

A direct comparison of the pressure dependence of T_c (for $H = 0$ T) with those of T_m

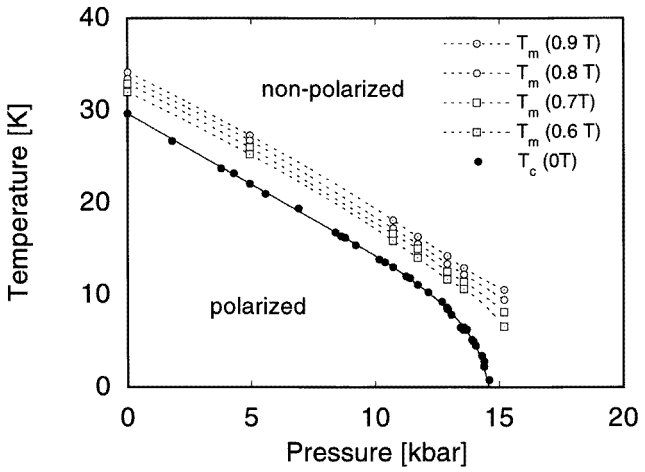

Figure 6. Comparison of the pressure dependence of T_c at zero field with those of T_m at fields from 0.6 T to 0.9 T. The pressure dependences are essentially the same for all fields studied here. The data on the variation of T_c with pressure were taken from reference [11].

at 0.6 T, 0.7 T, 0.8 T, and 0.9 T is shown in figure 6. The data on $T_c(P)$ shown here were taken from reference [11]. The pressure dependence of T_m is thereby remarkably analogous to that of T_c. In addition we note, for intermediate fields below 0.6 T, the collapse of the spiral shifts to lower T for increasing P. In the temperature versus pressure plane, properties below T_m now correspond to the field-polarized regime, and properties above T_m to the non-polarized regime.

4. Discussion

The discussion of the dependence of χ on temperature, pressure, and field may be divided into two parts. At first we address the effect of the field on global features of the magnetic state, for which we observe a crossover that may be taken as evidence of a field-induced spontaneous polarization of the itinerant-electron liquid. Secondly, details of the spiral state at low fields are discussed, which suggest that careful fine tuning stabilizes a re-entrant phase pocket in the close vicinity of P_c.

Features of the itinerant *ferro*magnetism in MnSi may be quantitatively accounted for by a self-consistent Ginzburg–Landau approximation [5, 11, 14]. The magnetic contribution to the free energy is here expanded to fourth order in terms of the time- and space-dependent magnetization. This model may be evaluated with the help of a few experimentally transparent, phenomenological parameters that may be related to the bare parameters of the non-interacting single-electron system through renormalization by the spectrum of thermal magnetic fluctuations. The value of T_c is then understood as being suppressed from its Stoner value by the strongly enhanced spectrum of thermal magnetic fluctuations. The temperature dependence of the mean fluctuation amplitude $\langle m^2 \rangle$, which is related to the imaginary part of the dynamical susceptibility through the quantum fluctuation-dissipation theorem [1, 5], accounts quantitatively for among other properties the large effective Curie moment above T_c and the anharmonic field dependence of the magnetization at high field and low T.

The self-consistent Ginzburg–Landau model referred to above may be taken as the

Hartree approximation of a more general Ginzburg–Landau–Wilson analysis of zero-temperature (i.e. quantum) phase transitions of itinerant-electron magnets [22]. This contrasts, for example, with the ($n \geqslant 4$)-component classical Ginzburg–Landau–Wilson description of complex *antiferro*magnetic phase transitions [23].

At ambient pressure, we interpret the low-field regime above T_m as an essentially non-polarized state, of which the nearly field-independent effective Curie moment provides 'fingerprint' evidence. In contrast, below T_m and at high field, the susceptibility varies as expected of a field-polarized state. It is remarkable that the crossover at T_m between these two extremes is not gradual, but well defined. The origin of the crossover line may be sought in its dependence on pressure and temperature. At ambient pressure the transition temperature T_m increases with field, as is qualitatively expected of an effect related to a thermally increasing fluctuation amplitude. With increasing pressure, the spectrum of magnetic fluctuations is on the other hand enhanced, and T_c collapses to zero. However, as previously reported, the transition crosses from second to weakly first order near P_c, and the paramagnetic susceptibility develops a broad peak at around $T^* \approx 12$ K [11]. The origin of this peak was explained on the basis of a deep minimum of the single-electron band structure giving rise to a negative quartic contribution to the Ginzburg–Landau expansion. For stability, the free energy must then be expanded to sixth order. The effect of low fields on the maximum at T^* may finally be pictured as inducing a spin splitting of the single-electron density of states that is small in comparison to the smearing by thermal magnetic fluctuations, thus causing a weak decrease of the peak at T^* as shown in figure 5.

It appears likely that the same deep minimum of the single-electron density of states is also at the heart of the field-induced crossover at T_m as suggested by a previous analysis [24]. However, a complete self-consistent computation of the higher-order coupling terms is difficult to evaluate, due to the lack of a precise understanding of the implicit dependence of the mean fluctuation amplitude $\langle m^2 \rangle$ on the static magnetization. In principle, a number of other mechanisms not related to the single-electron band structure may also give rise to a negative quartic contribution. They are (i) magneto-volume coupling, (ii) screening of the mode–mode coupling, or (iii) non-linear precession of the magnetization under the action of the molecular field [14, 25]. The effects of zero-point fluctuations of the local magnetization are, finally, also important, and may formally be included in the bare expansion parameters of the non-interacting system [5, 26]. However, their field dependence is not expected to account for the features observed here.

A field-induced change of curvature of the magnetization has also been reported for other representatives of itinerant d-electron magnetism, namely the cubic Laves phases $Y(Co, Al)_2$ and $Lu(Co, Al)_2$ [15, 16]. By comparison to MnSi, however, these materials show similar phenomena only at ultrahigh pulsed fields of up to 100 T.

We may now turn to the pressure dependence of the spiral state and its role in the magnetic phase diagram. The rather small change of H_{c2} under pressure suggests that its wavelength hardly changes. This is consistent with preliminary neutron diffraction studies under pressure [4, 21]. We conjecture therefore that MnSi as function of pressure is *not* driven towards *antiferro*magnetism, and that the approximation of an essentially *ferro*magnetic system remains useful for accounting for global features of the magnetic phase diagram.

An important detail of the spiral regime is, moreover, that it may be tuned to become a re-entrant magnetic phase closely above P_c. Qualitatively similar properties are also observed for f-electron systems belonging to the class of heavy-fermion materials such as $CeRu_2Si_2$. By comparison to MnSi, $CeRu_2Si_2$ has characteristics corresponding to an effective pressure 3 kbar above P_c. Systematically replacing Ce with La leads to a reduction

of the unit-cell volume, i.e. an effective negative pressure, which induces a complicated *antiferro*magnetically ordered state in $Ce_{1-x}La_xRu_2Si_2$ for $x > 0.08$. However, no re-entrant magnetism has been detected in these systems, as discussed in a recent review [27]. It is also worthwhile mentioning that experiments under pressure on $Ce_{0.8}La_{0.2}Ru_2Si_2$ ($P_c = 4$ kbar) show a weak pressure dependence of a 'conventional' metamagnetic transition. In view of the variety of mechanisms that may principally be at the heart of metamagnetic behaviour in itinerant-electron systems, we note that in these Ce compounds the effects of magnetostriction and zero-point fluctuations are strong. For instance, in pure samples of $CeRu_2Si_2$, a large expansion of the volume appears at the so-called pseudo-metamagnetic field H_m, driving the system towards a magnetic instability which is not reached even at the lowest temperatures. Properties of the ultrasound attenuation, thermal expansion, and forced magnetostriction in MnSi at ambient pressure [28, 29] provide evidence that these effects have to be taken into account for a more accurate description. Recent studies of the specific heat and forced magnetostriction of the anomaly observed at T_m at ambient pressure will be discussed elsewhere [30].

The determination of the magnetic phase diagram of MnSi is, finally, also important to an understanding of the metallic state from the point of view of the spectrum of fermion quasiparticle excitations. It was previously established that the quadratic T-dependence of the resistivity in the weakly spin-polarized (ordered) phase at ambient pressure is that anticipated of a conventional Fermi liquid. However, at P_c, the temperature dependence of ρ is always less than quadratic, and is accurately consistent with quasiparticle interactions arising from the virtual exchange of dispersive spin fluctuations down to the lowest temperatures investigated. Preliminary measurements show a return of the T-dependence of ρ at P_c towards a quadratic behaviour at constant fields for $H > H_m$ [20]. This is consistent with our interpretation that T_m and H_m mark the separation between an essentially non-polarized and a field-polarized magnetic phase.

In summary we have observed that the magnetic phase diagram of MnSi includes a well defined, strongly pressure-dependent crossover between a non-polarized and a field-polarized regime. The spin or fan spiral state appears to be supported *only* in the field-polarized regime, so a small pocket of a re-entrant phase exists near P_c in the field-polarized regime. The crossover at T_m may alternatively be interpreted as a change of the effective-quasiparticle interaction potential, separating between a conventional, highly renormalized Fermi liquid in the polarized regime and a *marginal* Fermi liquid with a quasiparticle interaction potential arising from the exchange of nearly critical spin fluctuations.

Acknowledgments

We would like to thank G G Lonzarich for suggesting this project, and the use of the high-purity single crystal of MnSi, originally grown for an earlier study of the de Haas–van Alphen effect [3]. CP would like to thank B Lebech and S M Hayden for discussing their neutron diffraction results prior to publication. Help from G Lapertot and M Couach in performing the experiments, and discussions with N R Bernhoeft, G J McMullan, and S R Julian are gratefully acknowledged. This work was made possible in part by grants from the Commission of the European Community.

References

[1] Ishikawa Y, Noda Y, Uemura Y J, Majkrzak C F and Shirane G 1985 *Phys. Rev.* B **31** 5884
[2] Bloch D, Voiron J, Jaccarino V and Wernick J H 1975 *Phys. Lett.* **51A** 259

[3] Taileffer L, Lonzarich G G and Strange P 1986 *J. Magn. Magn. Mater.* **54–57** 957
[4] Brown S A 1990 *PhD Thesis* University of Cambridge
[5] Lonzarich G G and Taileffer L 1985 *J. Phys. C: Solid State Phys.* **18** 4339
Lonzarich G G 1986 *J. Magn. Magn. Mater.* **54–57** 612
[6] Moriya T 1985 *Spin Fluctuations in Itinerant Electron Magnetism* (Berlin: Springer)
[7] Bak P and Jensen M H 1980 *J. Phys. C: Solid State Phys.* **13** L881
[8] Lebech B 1993 *Recent Advances in Magnetism of Transition Metal Compounds* (Singapore: World Scientific)
[9] Ishikawa Y, Shirane G, Tarvin J A and Kohgi M 1977 *Phys. Rev.* B **16** 4956
[10] Lebech B, Harris P, Skov Pedersen J, Gregory C I, Mortensen K, Bernhoeft N R, Jermy M and Brown S A 1995 *J. Magn. Magn. Mater.* **140–144** 119
Gregory C I, Lambrick D B and Bernhoeft N R 1992 *J. Magn. Magn. Mater.* **104–107** 689
[11] Pfleiderer C, McMullan G J, Julian S R and Lonzarich G G 1997 *Phys. Rev.* B **55** 8330 and references therein
[12] Julian S R, Pfleiderer C, Grosche F M, Mathur N D, McMullan G J, Diver A J, Walker I R and Lonzarich G G 1996 *J. Phys.: Condens. Matter* **8** 9675
[13] Fawcett E, Maita J P and Wernick J H 1970 *Int. J. Magn.* **1** 29
[14] Lonzarich G G 1996 *The Electron* ed M Springford (Cambridge: Cambridge University Press) and references therein
Lonzarich G G 1994 *Magnetic Phase Transitions at Low Temperatures* unpublished lectures
[15] Duc N H 1994 *J. Magn. Magn. Mater.* **131** 224
[16] Goto T, Aruga Katori H, Sakakibara T, Mitamura H, Fukamichi K and Murata K 1994 *J. Appl. Phys.* **76** 6682
[17] Flouquet J, Kambe S, Regnault L P, Haen P, Brison J P, Lapierre F and Lejay P 1995 *Physica* B **215** 77
[18] See, e.g.,
Izyumov Y A 1984 *Sov. Phys.–Usp.* **27** 845 and references therein
[19] Pfleiderer C 1997 *Rev. Sci. Instrum.* **68** 1532
[20] Thessieu C 1995 *PhD Thesis* Université de Paris IV
Thessieu C, Flouquet J, Lapertot G, Stepanov A N and Jaccard D 1995 *Solid State Commun.* **95** 707
[21] Sorensen S A and Lebech B 1996 *Riso National Laboratory Report* Riso-R-863(EN)
[22] Millis A J 1993 *Phys. Rev.* B **48** 7183
[23] See, e.g.,
Mukamel D and Krinsky S 1976 *Phys. Rev.* B **13** 5065
[24] Yamada H 1993 *Phys. Rev.* B **47** 11 211
[25] McMullan G J 1989 *PhD Thesis* University of Cambridge
[26] Takahashi Y and Sakai T 1995 *J. Phys.: Condens. Matter* **7** 6279
[27] Haen P, Lapierre F, Voiron J and Flouquet J 1996 *J. Phys. Soc. Japan Suppl.* B **65** 27 and references therein
[28] Kusaka S, Yamamoto K, Komatsubara T and Ishikawa Y 1976 *Solid State Commun.* **20** 925
[29] Matsunaga M, Ishikawa Y and Nakajima T 1982 *J. Phys. Soc. Japan* **51** 1153
[30] Pfleiderer C, Calemzuck R and Bernhoeft N R 1997 unpublished